

Structural properties of molten silicates from *ab initio* molecular-dynamics simulations: comparison between CaO-Al₂O₃-SiO₂ and SiO₂.

Magali Benoit and Simona Ispas
*Laboratoire des Verres, Université Montpellier II,
 Place E. Bataillon, 34095 Montpellier, France*

Mark E. Tuckerman
*Department of Chemistry and Courant Institute of Mathematical Sciences,
 New York University, New York, NY 10003 USA*
 (October 24, 2018)

Abstract

We present the results of first-principles molecular-dynamics simulations of molten silicates, based on the density functional formalism. In particular, the structural properties of a calcium aluminosilicate [CaO-Al₂O₃-SiO₂] melt are compared to those of a silica melt. The local structures of the two melts are in good agreement with the experimental understanding of these systems. In the calcium aluminosilicate melt, the number of non-bridging oxygens found is in excess of the number obtained from a simple stoichiometric prediction. In addition, the aluminum avoidance principle, which states that links between AlO₄ tetrahedra are absent or rare, is found to be violated. Defects such as 2-fold rings and 5-fold coordinated silicon atoms are found in comparable proportions in both liquids. However, in the calcium aluminosilicate melt, a larger proportion of oxygen atoms are 3-fold coordinated. In addition, 5-fold coordinated aluminum atoms are observed. Finally evidence of creation and annihilation of non-bridging oxygens is observed, with these oxygens being mostly connected to Si tetrahedra.

PACS numbers: 61.20.Ja, 71.15.Pd, 91.60.-x, 61.43.Fs

1. INTRODUCTION

Silicate melts are the precursors to industrially and technologically important materials including ceramics and nuclear and industrial waste confinement glasses. They also occur naturally in the form of geologic magmas. Despite their technological relevance and geophysical importance, however, their microscopic characteristics are not well understood [1]. The primary reason for this is that the structure of the melt is far more difficult to characterize than that of crystalline silicates, necessitating a combination of indirect methods. Most of the information about the liquid structures come from extrapolations of studies of glasses [2–13], but large changes in properties, such as heat capacity, thermal expansion, compressibility, etc., as a result of heating suggest significant structural changes with increasing temperature [14–16].

In recent years, theoretical studies based on classical molecular-dynamics (MD) simulations have been able to treat binary or ternary silicate systems with reasonable success. However, accurate and reliable descriptions of systems containing more than three different atomic species by classical MD methods has proved far more difficult, although several studies have been able to predict general trends that are consistent with experimental results [17–21]. This problem is particularly acute when cations such as Na^+ or Ca^{2+} are introduced in silicate glasses, as it is generally difficult to find interatomic potentials that can accurately treat both the covalent and the ionic nature of the interactions and are also capable of describing the bond breaking and forming events that can occur in such chemically diverse environments. These difficulties can be circumvented by employing the *ab initio* molecular dynamics method, in which internuclear interactions are calculated “on the fly” from electronic structure calculations. Indeed, recent *ab initio* MD studies of silica glass and of its melt have demonstrated the ability of this approach to describe the local structure and dynamics of such systems with reasonable accuracy. These studies have also highlighted the advantages of employing a method which, additionally, allows direct access to the *electronic* properties of the system [22,23].

It is well known that many important macroscopic properties of silicate melts, such as the viscosity, the glass transition temperature T_g , or the resistance to chemical change, for example via corrosion, are dramatically altered by changes in the composition [1,14,18]. For instance, introduction of Na^+ ions into a SiO_2 melt causes the viscosity at a given T_g/T ratio to decrease by several orders of magnitude from that of the pure SiO_2 [1]. The presence of cations such as Na^+ , K^+ , Ca^{2+} or Mg^{2+} , known as network modifier cations, induces such changes by breaking some fraction of the Si-O bonds thereby creating non-bridging oxygens and disrupting the tetrahedral silicate network. Non-bridging oxygens (NBO) are oxygen atoms which do not connect two tetrahedral cations or network-forming atoms, such as Si. Non-bridging oxygens provide relatively weak connections between the network forming atoms and the network modifier cations. However, when other network-forming atoms such as aluminum are introduced into the system, there is a gradual conversion of non-bridging oxygens into bridging oxygens. This arises from the fact that most of the Al atoms are tetrahedrally coordinated (AlO_4^-), and the resulting negative charge compensates the positive network modifier cation charge. In such cases, non-bridging oxygens can be created and the network broken only if there is an *excess* of network modifier cations, and it is for this reason that the viscosity of ternary liquids, such as CaSiO_3 or Na_2SiO_3 , progressively

increases as the network modifier oxide (CaO or Na_2O) is replaced by Al_2O_3 . The conventional explanation for the increase in viscosity is the transformation of non-bridging oxygens into bridging oxygens as the concentration of Al_2O_3 is increased. Generally, the number of NBO can be predicted based on a knowledge of the composition by simple stoichiometric arguments. However, it has recently been shown that such simple stoichiometric predictions are not exactly fulfilled in calcium aluminosilicate (CAS) glasses and that a small proportion of NBO can be present even if all the modifier cations should, in principle, exactly compensate the AlO_4^- tetrahedra [12,13].

In this paper, the results of an *ab initio* molecular-dynamics simulation of a calcium aluminosilicate (CAS) melt are presented and its microscopic characteristics are compared to those of a pure silica melt. To our knowledge, these are the first fully *ab initio* MD studies of the CAS melt. We have chosen a $\text{CaO-Al}_2\text{O}_3\text{-SiO}_2$ system with a composition as close as possible to the basic composition of the confinement matrix for the nuclear wastes. This system also possesses a local structure close to those of some rapid cooling magmas. The chosen composition contains more Ca^{2+} ions than are needed to compensate the AlO_4^- tetrahedra, thus leading to the formation of non-bridging oxygens. By carrying out a comparative study of the CAS and pure silica melts, it is possible to describe the detailed modifications in the network due to the presence of Al and Ca^{2+} in the system.

This paper is organized as follows: In Sec.2, the *ab initio* methodology is briefly described and the details of the particular simulations performed here are given. In Sec.3, main results of the comparative study are presented, including structural properties of the CAS and silica systems. These results are discussed in Sec.4 and conclusions are given in Sec.5.

2. SIMULATION DETAILS

Equilibrated configurations of the two liquids were generated by classical molecular dynamics runs, the details of which are described in Secs. 2 A and 2 B below, and were subsequently used to initialize the *ab initio* MD simulations. The two systems were then equilibrated within a Car-Parrinello (CP) *ab initio* MD run [24] performed with the *ab initio* MD code, CPMD [25]. In the *ab initio* MD simulations, the electronic structure was treated via the Kohn-Sham (KS) formulation of density functional theory [26] within the local density approximation for the pure silica system and within the generalized gradient approximation for the CAS system employing the B-LYP functional [27,28]. The KS orbitals were expanded in a plane-wave basis at the Γ -point of the supercell up to an energy cutoff of 70 Ry for both systems. Core electrons were not treated explicitly but were replaced by atomic pseudopotentials of the Bachelet-Hamann-Schlüter type for silicon [29] and the Troullier-Martins type for oxygen [30]. A Goedecker-type pseudopotential [31] was employed for aluminum, and a Goedecker-type semi-core pseudopotential was employed for calcium. The choices of the pseudopotentials, exchange and correlation functionals and plane-wave cutoff are justified by previous studies carried out on amorphous SiO_2 [23] as well as total energy calculations carried out on small molecules (see Table I).

A. Molten SiO₂

The molten silica system contains 26 SiO₂ units in a cubic box of edge length 10.558 Å, which corresponds to a mass density of 2.2 g·cm⁻³. The density of the glass was chosen so that the configurations could later be used in quenching runs to generate glass structures. Although the density is, therefore, a little too high compared to the real liquid, it is not expected that this will significantly affect our findings, which are based on the comparison of network and disrupted network systems. The SiO₂ initial configuration was obtained by melting a 216 SiO₂ units β -cristobalite crystal at 7000 K with classical molecular dynamics using the van Beest, Kramer and van Santen (BKS) potential [35,36] and then cooling it to 4200 K using the same potential. At this temperature, a cubic box of edge length 10.558 Å and containing 26 SiO₂ was extracted from the 216 SiO₂ system and equilibrated during \sim 35 ps.

The classically equilibrated SiO₂ liquid configuration was further equilibrated within a 6-ps *ab initio* MD run at 4200 K using a time step of 0.096 fs, then quenched to 3500 K at a quench rate of $3 \cdot 10^{15}$ K·s⁻¹ with the same time step, and finally equilibrated at 3500 K for 6 ps using a time step of 0.108 fs. In order to achieve rapid equilibration and efficient canonical sampling of the system, a separate Nosé-Hoover chain thermostat [37] was placed on each ionic degree of freedom (known as “massive” thermostating [38]) and an additional Nosé-Hoover chain thermostat was placed on the electronic degrees of freedom [37,39]. In all cases, a fictitious electronic “mass” parameter, μ (having units of energy×time²) of 600 a.u. was employed.

B. Molten calcium aluminosilicate

The CAS system contains 22 SiO₂, 4 Al₂O₃ and 7 CaO, which gives approximately 67 %, 12 % and 21 % molar percentages of these units, respectively, and a total of 100 atoms. For this particular composition, there are 8 Al atoms which give rise to 8 AlO₄⁻ tetrahedra under the assumption that all Al atoms form tetrahedra. Four of the Ca²⁺ ions then compensate the negative charges of the AlO₄⁻, leaving three Ca²⁺ that can break the network and create, ideally, 6 non-bridging oxygens. The system is confined in a cubic box with an edge length of 11.3616 Å, which corresponds to a mass density of 2.4 g·cm⁻³. This density has been chosen by extrapolating to 2500 K the data obtained by Courtial and Dingwell for a system of close composition [14]. For this case, classical MD simulations were also carried out on systems containing 100 and 5184 atoms with the same composition described above. By comparing the structural properties obtained from the classical MD simulations at the two system sizes, it was possible to estimate the finite-size effects on the *ab initio* MD data and to validate the choice of the system size for the *ab initio* simulations [40].

The initial configuration of the CAS system for the *ab initio* MD simulation was generated using a Born-Mayer-Huggins potential [19] in a classical MD run to obtain a melt at 2000 K. The CAS liquid was then heated to 2300 K with CPMD and further equilibrated for 2 ps using a time step of 0.12 fs and an electron mass parameter of 800 a.u. It was then heated again to 3000 K and equilibrated for 6.8 ps, during which stronger diffusion effects occurred than at the lower temperature. Again, rapid equilibration and efficient canonical sampling

was achieved by coupling a Nosé-Hoover chain thermostat [37,39] to each ionic degree of freedom.

3. PRESENTATION OF RESULTS

In this section, the structural properties of the CAS and SiO_2 melts are presented in terms of network pair correlation functions, angle distributions, examination of Al-O-Al linkages, proportion of NBO, and cation pair correlation functions. A full discussion of these results is presented in Sec. 4.

A. Network pair correlation functions

In this subsection, the pair correlation functions (PCF) corresponding to the network-forming atoms (Si, O and Al for CAS) are presented for the CAS melt and compared to those of the silica melt when appropriate.

The Si-O PCF and the corresponding integrated coordination number are almost identical for the two systems, which confirms that the basic tetrahedral unit is conserved between these two liquids (Fig. 1(b)). Moreover, the similarity in CAS between the Al-O (Fig. 1(d)) and Si-O PCFs is clear evidence of the fact that the Al atoms can substitute for the Si atoms at the center of the tetrahedra. The ability of Al to replace Si in the network has also been observed in experimental studies of aluminosilicate glasses [7–11]. The slight shift of the Al-O peak to a higher r value is consistent with previously observed and calculated Al-O and Si-O bond lengths in aluminosilicates [2] as well as with the larger covalent radius of Al compared to Si.

Comparison of the Si-Si and O-O PCFs between the CAS and SiO_2 liquids also shows a slight shift of the first peak toward higher r values in the CAS case, and the plateau in the running Si-Si coordination number is considerably lower in the CAS system. In order to explain the shift in the Si-Si peak, we first note that in silica, the first Si-Si neighbors correspond to neighboring tetrahedra (i.e. the first Si-Si distances correspond to the Si-O-Si linkages). In the CAS system, however, some of the oxygens, in particular, the NBO, are connected to only one network forming atom (Si or Al) and one network modifier (Ca), thus forming Si-O-Ca or Al-O-Ca linkages. Therefore, some of the first-neighbor Si-Si distances are due to these more complex linkages. The reduction in the Si-Si coordination is due primarily to the fact that some of the Si atoms are replaced by Al atoms. As a result of the Al substitution for Si *and* the presence of NBOs, there are fewer direct Si-O-Si linkages in CAS, leading to an average coordination of 2.4 compared to 4 in the pure silica system. The shift in the position of the first O-O peak in the CAS system is simply a reflection of the fact that the Al-O bond length is larger than that of Si-O. Thus, if Al substitutes for Si, maintaining both the regular tetrahedral coordination and the angles between neighboring tetrahedra as in silica, then the observed shift in the O-O peak is expected.

B. Angles distributions

Evaluation of the angles distributions and coordination numbers presented in this subsection was based on distance cutoffs determined from the first minimum of the PCFs (2.38 Å for Si-O and 2.56 Å for Al-O).

In order to investigate the effect of Al substitution for Si on the tetrahedral angles, the distributions of the O-Al-O and the O-Si-O angles for both systems were computed and are shown in Fig. 2. The figure shows that the O-Al-O distribution in CAS is somewhat broader than the O-Si-O distribution in both CAS and in silica. The mean values of these distributions, however, are very similar ($108.8^\circ \pm 15$ for O-Si-O in CAS, $108.3^\circ \pm 17$ for O-Si-O in SiO₂ and $107.6^\circ \pm 21$ for O-Al-O), suggesting that the angles between tetrahedra remain approximately unchanged upon Al substitution. Therefore, the primary cause of the shift in the first peak of the O-O PCF is the increased Al-O bond length.

The relative broadness of the O-Al-O angle distribution compared to that of O-Si-O likely signifies an Al-O coordination that is different from 4. In order to check this assertion, the average oxygen coordination of the Al and Si atoms was computed. The histogram of the number of oxygen neighbors of Al and Si is shown in Fig. 3 (left panel). From the figure, it can be seen that, although Al substitutes for Si in the network, the fraction of 3-fold and 5-fold coordinated Al exceeds that of Si. Recent high-temperature NMR measurements of aluminosilicate melts [16,41] directly revealed the presence of 6-fold coordinated Al and strongly suggested the possibility of 5-fold coordinated Al, although the latter were not directly observed in these experiments. However, MAS NMR experiments [42,43] have provided clear evidence of the existence of small amounts of both 5- and 6-fold Al coordination in binary Al₂O₃-SiO₂ and in ternary CaO-Al₂O₃-SiO₂ glasses [42,43]. Indeed, the average proportion of 5-fold coordinated Al in the present simulations is also small compared to 4-fold coordinated Al. However, we observe less than 1 % of 6-fold coordinated Al for this particular composition.

We also investigated the effect of the Al substitution for Si on the angles between neighboring tetrahedra. The Si-O-Al and Si-O-Si angles distributions were computed for the CAS melt and compared to the Si-O-Si angle distribution for the SiO₂ melt (Fig. 4). The Si-O-Si distributions are very similar in the two systems, only showing a slight difference in the intensity of the shoulder around 90° - 100° . It can be shown that values of the Si-O-Si angles around 90° - 100° can be attributed to 2-membered rings and/or to oxygen tri-clusters, oxygens bound to three network-forming atoms (see Sec. 4). A comparison of the proportions of these units in the two different systems is consistent with the differences observed in the angle distributions and will be discussed in more detail in section 4. In CAS, the Si-O-Al angle distribution shows a higher shoulder around 90° - 100° than the Si-O-Si one. Again the Si-Al 2-membered rings and the oxygen tri-clusters are at the origin of this shoulder. Overall, the introduction of Al and Ca does not significantly affect the Si-O-Si angle distribution in the molten state.

C. Al-O-Al linkages

Although the Al-Al PCF (Fig. 1(e)) is somewhat noisy due to the small number of Al atoms in the system, this correlation function exhibits a first peak at ~ 3.2 Å, which

indicates that some Al-O-Al linkages are present in the system. This would appear to be in direct violation of the so called Al avoidance principle or Löwenstein’s rule [44], an empirical rule which states that two Al tetrahedra are never found linked by an oxygen atom in aluminosilicate crystals and glasses, at low Al content. However this rule has been found experimentally not to be exactly fulfilled in some glasses and melts, *in particular* when Ca atoms are present, leading to Al/Si alternance disorder [45–47].

The degree of Al avoidance violation can be quantified by examining the average number of Al-O-Al linkages formed over the course of the simulation. By computing the number of Al atoms around each oxygen atom (using the first minimum of the $g(r)$, 2.56 Å, as the Al-O cutoff distance) and counting one Al-O-Al linkage when two Al atoms are found, an average value of 2.26 Al-O-Al linkages is obtained, i.e., $\approx 57\%$ of Al atoms form Al-O-Al linkages, if they do not form chains. Moreover, half of the oxygen atoms involved in the Al-O-Al linkages are found to be 3-fold coordinated, on average. The proportion of Al-O-Al linkages is greater than that which would be obtained from a purely random model [46]. Thus, the Al atoms appear to favor Al-O-Al linkages in the CAS liquid and adhere only minimally to the Al avoidance principle. That the presence of Ca^{2+} cations preferentially favor Al-O-Al linkages and, thus, strong violation of the Al avoidance principle, has also been suggested by static *ab initio* calculations of clusters [48] and is likely due to the greater aggregation of negative charge around the Al-O-Al linkage. In a disordered (liquid or glass) state, the relatively large Ca^{2+} charge is, therefore, able to induce formation of such linkages.

D. Non-bridging oxygens

In the present CAS system, stoichiometry dictates that four of the Ca^{2+} ions should compensate the eight aluminum tetrahedra (assuming all the Al are four-fold coordinated), leaving three Ca^{2+} cations to create six non-bridging oxygens. The number of NBOs in the system can be computed by counting the number of oxygen atoms which have only one Si or Al neighbor and one Ca neighbor. The neighbors are defined to be any atoms within a sphere of radius determined by the first minimum of the corresponding PCF (2.38 Å for O-Si, 2.56 Å for O-Al, and 3.40 Å for O-Ca – see Sec. 3A and Sec. 3E), centered on each oxygen atom. The distribution of the number of non-bridging oxygens found in the CAS system during the simulation is depicted in Figure 5. The distribution is peaked at 9, while the probability of the system’s possessing six NBOs is relatively small. Thus, the average number of NBOs in the system is larger than would be predicted from a simple stoichiometric argument. In a recent experiment of Stebbins and Xu [12], it was found that in a particular CAS glass system in which the Ca^{2+} ions perfectly compensate all of the negative Al tetrahedra, some NBOs are present, although stoichiometric arguments would predict that there should be none. Since the present study is concerned with the liquid state, where bond-length fluctuations and other dynamical effects are more significant than in the glass, we cannot directly compare our result with that of Stebbins and Xu. However, given that the trend is toward a *larger* number of NBOs in the glass than the stoichiometry would predict, the fact that our calculations predict a similar trend in the liquid accords well with the experimental result.

In Figure 6, we present the first peaks of the PCFs between the oxygen atoms and the network-forming atoms (Si and Al), evaluated separately for bridging (BO) and non-bridging

(NBO) oxygen atoms. The maximum intensity of the X-BO and X-NBO (X=Si,Al) peaks are located at different r values, the X-NBO distances being shorter than the corresponding to those for X-BO. This result is in agreement with experimental results concerning sodium silicates and aluminosilicates [2,49] and with *ab initio* calculations on clusters [48,50]. In the simulated CAS melt, the most probable distances are $r(\text{Si} - \text{BO}) \approx 1.64 \text{ \AA}$ and $r(\text{Si} - \text{NBO}) \approx 1.58 \text{ \AA}$, $r(\text{Al} - \text{BO}) \approx 1.75 \text{ \AA}$, and $r(\text{Al} - \text{NBO}) \approx 1.70 \text{ \AA}$. It is also interesting to note that the Si-O and Al-O distances in the molten state are very close to their respective values in the glass.

E. Calcium pair correlation functions

In this subsection, structural properties involving the calcium atoms in the CAS melt, such as PCFs and coordination numbers, are presented.

The calcium PCFs are depicted in Fig. 7. The Ca-O radial distribution function (Fig. 7(b)) exhibits a first peak at approximately 2.33 \AA , in agreement with experimental values obtained for glasses and minerals of similar composition [3,9]. The coordination of calcium atoms is found to be equal to 6.2 ± 1.3 on average (see Fig. 8), while the experimental value in calcium aluminosilicate *glasses* is estimated to be between 5 and 6 [3,9]. This comparison is only meant as a qualitative one, since direct comparison between the liquid and glass states is not possible. Indeed, the high temperature of the molten state gives rise to large fluctuations in the Ca-O coordination number.

The Ca-Si and Ca-Al PCFs ((Fig.7(a) and (c)) also show well defined first peaks at $\sim 3.45 \text{ \AA}$, which are due either to direct bonds with non-bridging oxygens, i.e., Si-O-Ca and Al-O-Ca linkages, or to the proximity of Ca^{2+} ions to compensate the negative AlO_4^- groups. It can be shown that the Ca-Si peak is due to the former and the Ca-Al to the latter. Indeed, we observe mostly Si-NBO bonds and very few Al-NBO bonds ($\sim 91 \%$ of the NBOs are connected to Si atoms), a result that is consistent with recent X-ray experiments on glasses of similar composition [9]. In Fig. 6, in which PCFs are evaluated separately for bridging (BO) and non-bridging (NBO) oxygen atoms, we observe that Si PCFs possess similar characteristics for both BO and NBO. In contrast, the Al-NBO PCF is generally small compared to the Al-BO PCF, which indicates that almost all the NBO atoms are connected to Si tetrahedra. Thus, the first peak in the Ca-Al PCF is due to nearby Ca^{2+} ions which, in this close proximity, are able to compensate the negative AlO_4^- groups. Note that the Ca-Ca PCF, shown in Fig. 7(d) does not exhibit a well defined first peak, which suggests that at liquid conditions, there is no ordering of the network modifier cations.

4. DISCUSSION

In order to explain the presence of excess non-bridging oxygens, Stebbins and Xu [12] proposed two possible structural units: AlO_5 groups and tri-clusters. Tri-clusters are oxygen atoms bonded to three network-forming atoms, either Al or Si, and they can be of four types : oxygens bonded to three silicon atoms (3 Si), to two silicon and one aluminum atoms (2 Si - 1 Al), to one silicon and two aluminum atoms (1 Si - 2 Al), and to three aluminum atoms (3 Al). In the molten state we observed that the fraction of 3-fold coordinated oxygen atoms

is not negligible. A more detailed analysis of these tri-clusters in CAS showed that, due to the small number of aluminum atoms in the system, 3-Al tri-clusters are absent and that the most numerous tri-clusters are the 2 Si - 1 Al and 2 Al - 1 Si. When added together and averaged over the trajectory, the percentage of oxygen atoms forming tri-clusters is around 6.9 % in the CAS system, with large fluctuations of about ± 2.8 %. This result accords well with the idea of Stebbins and Xu [12] that a given number of oxygen tri-clusters should be present in the glass in order to compensate the formation of the non-bridging oxygens. It could be argued that the relatively small number of tri-clusters may be a consequence of thermal fluctuations at liquid conditions. Although thermal induced tri-cluster formation cannot be ruled out, it is worth noting that only 4.7 % of tri-clusters could be identified in the silica melt at higher temperature.

On the other hand, in CAS, we also find a relatively high number of AlO_5 units: on average, approximately ~ 1.9 or 23% of Al are 5-fold coordinated, however the fluctuations are such that in any configuration, anywhere between 0 and 3 AlO_5 units may exist. This result suggests that the presence of highly coordinated aluminum atoms could favor the creation of excess NBO atoms. Most experimental studies [8–11] only show evidence of 4-fold coordinated aluminium atoms in aluminosilicate glasses. However, as discussed in Sec.3B, experimental evidence of higher Al coordination numbers (mainly 5 and 6-fold) in the glass and molten state of calcium aluminosilicate systems exists, and, recently, evidence of high Al coordination in magnesium aluminosilicate glasses has been reported [14,16,41–43].

In Fig. 5, we present the distribution of the number of NBOs found during the simulation of the CAS melt. The relatively large width of the distribution indicates that the identity of the oxygen atoms (BO or NBO) does not remain constant during the simulation. Indeed, bond-breaking events that lead to the creation and the annihilation of non-bridging oxygens, i.e. Q_4 and Q_3 exchanges, are observed. This mechanism has been suggested as underlying the induction of shear flow and, hence, a decrease in the viscosity in these systems [14–16]. Since almost no NBOs are found to be connected to Al atoms on average during the simulation (see Sec. 3E), it is highly probable that more Al-O bonds are broken than Si-O bonds. In silica, however, since there are no NBOs, a different mechanism must underly the flow process. Unfortunately, we can not extract direct dynamical quantities from the present simulations. This is mainly due to the fact that at high temperature in the molten state, the electronic gap is too small compared to $k_B T$ to ensure the decoupling of the ionic and the electronic degrees of freedom, which is needed for *ab initio* molecular dynamics in a constant energy ensemble. The use of thermostats becomes compulsory and the direct access to dynamical properties is no longer available. We are currently developing new techniques to treat this problem [51].

Nevertheless, the structural characteristics of the melt can give some insight into its dynamical properties. For instance, it has been suggested that five-coordinated network cations could act as transition states for the flow process [14–16,43]. This atomic-scale flow step was described in Ref. [13] as an oxygen atom changing from bridging to non-bridging, or vice versa: “A non-bridging oxygen bonded to a modifier cation can approach a silicon atom and make it over-coordinated. Dissociation of the over-coordinated SiO_5 results in an exchange of the roles of oxygen from bridging to non-bridging ...”. In the present simulations, we find a significant fraction of 5-fold coordinated silicon atoms (≈ 9.9 % in SiO_2 at 3500 K and ≈ 3.8 % in CAS at 3000 K) and a large fraction of 5-fold coordinated aluminum atoms

in CAS (see Fig.3). These numbers show very large fluctuations around their average values which supports the idea that these units participate in the transition state of the flow steps. The relatively large number of 5-fold coordinated network cations in CAS compared to SiO_2 , even at a lower temperature, could be a signature of a lower viscosity in the aluminosilicate melt. It is also interesting to note that the number of 5-fold coordinated Si atoms is larger in SiO_2 than in CAS. In the latter system, the 5-fold coordinated Al atoms, which are energetically more favorable, replace the 5-fold Si atoms as the transition state of the flow step.

In Sec. 3, it was seen that the local order in the two silicate melts is only slightly affected by temperature and by the introduction of a small number of modifier cations. The Si tetrahedral units remain the most probable basic units of the system, with probabilities of 85 % in SiO_2 and 89% CAS at 3000 K. From structural characteristics such as pair correlation functions or angle distributions, therefore, it is almost impossible to discern the disruption of the silicate network by the modifier cations, at high temperature. The effect can be seen, however, by looking at characteristic patterns in the network. An example is the oxygen-oxygen coordination number, which is a more sensitive probe of the network disruption. We have evaluated these coordination numbers by counting the number of oxygen neighbors around each oxygen atom inside a sphere of radius determined by the first minimum of the O-O radial distribution function. Histograms of the oxygen-oxygen coordinations are depicted in Fig. 9 for the two different systems. For SiO_2 at 3500 K, the distribution of the O coordination peaks around 7 or 8 atoms, which indicates that the oxygen atoms have more oxygen neighbors than would be expected from two connected tetrahedra. In the SiO_2 glass, in which the network is not broken, the maximum of the distribution occurs at 6 which corresponds to the number of oxygen neighbors belonging to two connected tetrahedra. The fact that, at 3500 K, the maximum is located between 7 and 8 in silica shows that part of the network has been broken. One of our hypotheses is that 2-membered rings and highly coordinated network formers are the cause of the increased number of oxygen neighbors. Indeed, the percentage of 2-membered rings in silica is not negligible at 3500 K (~ 12.4 %). It could be argued that our liquid silica system is too compressed (its density is equal to the experimental density of the silica glass at room temperature) and that the high pressure induces the shift in the O-O correlation and the large number of edge-sharing tetrahedra. However, results of classical-molecular dynamics on liquid silica at several densities and temperatures show that this is not the case [52,53]. At ≈ 3200 K and zero pressure, the O-O distribution resembles the distribution in Fig. 9 for silica [52] whereas at higher pressure (for a density of 2.35 g.cm^{-3}) and temperatures up to 4200 K, the O-O distribution is peaked between 6 and 7, which is close to that of the glass structure [53]. The shift of the O-O distribution with pressure is accompanied by a decreasing number of edge-sharing tetrahedra. This “non intuitive” behavior has already been seen in previous Monte Carlo simulations of liquid silica under pressure, in which it has been shown that the proportion of small rings decreases with increasing pressure [54]. Given the similarities between our result and that of Ref. [52], and given the small thermal expansion of silica ($0.54 \cdot 10^{-6} \text{ K}^{-1}$ at 1000°C [55]), it is clear that the high O-O correlation is a consequence of the high temperature of the system.

The distribution of O-O coordination in CAS at 3000 K is shifted towards higher numbers compared to that of SiO_2 (Fig. 9). In the former, the disruption of the network is not only

due to the NBOs but also to the presence of highly coordinated Al atoms which weaken the structure [18]. The CAS melt density is only slightly larger than that given by the extrapolation to 3000 K of experimental data [14], therefore the high correlation of the oxygen atoms is clearly due only to the high temperature. The relative shifts of the O-O distributions between the two different systems can be related to the disruption of the three dimensional network. In the two melts, thermal effects create defects such as 2-membered rings and SiO_5 units in comparable proportions. In CAS, however, the disruption of the network is also driven by the presence of non-bridging oxygens, which break some of the Si-O bonds, as well as by the presence of the aluminum atoms which possess high coordination numbers. Indeed, the presence of aluminum atoms has already been proven to be responsible for the increased fragility of the silicate network [18], which can be traced to the fact that the Al have broader coordination distributions, leading, therefore, to an increased flexibility of the network structure than in SiO_2 .

The use of the Nosé-Hoover chain thermostating method [37] in the present simulations allows the heat capacity at constant volume, C_v to be computed efficiently using the relation:

$$\Delta E = \sqrt{k_B T^2 C_v} \quad (1)$$

where $\Delta E = \sqrt{\langle E^2 \rangle - \langle E \rangle^2}$ denotes the fluctuations of the potential energy plus the kinetic energy of the ions over the course of the simulation. In silica at 3500 K, we find that the heat capacity at constant volume is equal to $91.5 \text{ J mol}^{-1} \text{ K}^{-1}$. As a first approximation, we can roughly estimate the difference between C_v and C_p , the heat capacity at constant pressure, which is the experimentally measured quantity:

$$C_p - C_v = TV \frac{\alpha^2}{\beta} \quad (2)$$

where α is the thermal expansion coefficient and β the isothermal compressibility. Using the experimental values $\alpha = 0.54 \cdot 10^{-6} \text{ K}^{-1}$, valid at 1000°C , and $\beta = 2.74 \cdot 10^{-2} \text{ GPa}^{-1}$ at 300 K [55], we find a difference of $C_p - C_v = 1.0 \cdot 10^{-3} \text{ J mol}^{-1} \text{ K}^{-1}$, so $C_p \approx 91.5 \text{ J mol}^{-1} \text{ K}^{-1}$. This value does not disagree with an extrapolation of the experimental values of C_p from Ref. [56] and is close to the values obtained by Scheidler *et al.* [57] from molecular dynamics simulation of the SiO_2 melt in the same temperature range, using the BKS potential [35]. Scheidler *et al.* computed the frequency dependent specific heat from $T=2750 \text{ K}$ up to $T=6100 \text{ K}$ and found a reasonable extrapolation of the experimental $C_p(T)$ above T_g .

For the CAS melt at 3000 K, we find a value of $C_v = 99.28 \text{ J mol}^{-1} \text{ K}^{-1}$ and an estimate of the difference, $C_p - C_v = 0.189 \text{ J mol}^{-1} \text{ K}^{-1}$, which gives $C_p \approx 99.47 \text{ J mol}^{-1} \text{ K}^{-1}$. The $C_p - C_v$ difference has been estimated using experimental values for calcium aluminosilicate systems of close compositions: $\alpha = 54.5 \cdot 10^{-7} \text{ K}^{-1}$ at 815°C (25 mol% CaO, 15 mol% Al_2O_3 , 60 mol% SiO_2) [58] and $\beta = 1.28 \cdot 10^{-2} \text{ GPa}^{-1}$ at 300 K (26.7 mol% CaO, 13.3 mol% Al_2O_3 , 60 mol% SiO_2) [55]. Although this estimate of C_p is relatively crude, it can be used to give an order of magnitude for C_p at high temperature. To our knowledge, no experimental values of C_p have been reported for a CAS system of close composition, at high temperature.

5. CONCLUSION

The structural properties of two different molten silicates have been analyzed using first-principles molecular-dynamics. It has been observed that, even in the calcium aluminosilicate melt, the basic structural unit of the system, i.e. the SiO_4 tetrahedron is not destroyed at high temperature and that the aluminum atoms can substitute for the silicon atoms in the center of the tetrahedra. Analysis of the structure of two melts show that the temperature effects induce the creation of 2-membered rings, 3-fold coordinated oxygen atoms and 5-fold coordinated silicon and aluminum atoms. In CAS, in particular, a relatively large proportion of Al atoms are found to be 5-fold coordinated.

In the CAS system, a larger number of non-bridging oxygens than would be predicted from stoichiometry was found. This excess of NBO is in agreement with recent experimental results on glasses of composition similar to the present composition [12] and is likely due to the presence of AlO_5 units as well as oxygen tri-clusters (mainly 2 Si - 1 Al). Also in the CAS system, it is found that the aluminum avoidance principle is violated and that most of the non-bridging oxygens are located on silicon tetrahedra, both results being in agreement with recent experimental data [9,45,46]. Finally, evidence of the creations and annihilations of non-bridging oxygens has been obtained. These processes likely play a key role in the flow mechanism in this system. A detailed understanding of the diffusion process, although extremely interesting, would require considerable computer time and would represent a methodological challenge for the *ab initio* approach. While we are currently developing new techniques to treat this problem [51], the study of the dynamical properties in these systems remains, for the present, beyond the scope of this paper. In addition, since it is not possible to determine which of the dominant structural motifs in CAS are a direct consequence of thermal fluctuations, we intend, as future work, to perform a quench of the CAS system to room temperature in order to study its structural properties in the glassy state.

ACKNOWLEDGMENTS

We would like to thank Dominique Ghaleb and Jean-Marc Delaye who initiated the CAS simulations and provided the classical initial sample, and Philippe Jund who provided the initial silica sample. Our warm thanks to Rémi Jullien, Walter Kob and Dominik Marx for very interesting and stimulating discussions and to Jürg Hutter for his invaluable help with the CPMD code. Concerning the CAS simulations, the work of M.B. was supported by a NATO grant. M.E.T would like to acknowledge support from NSF CHE-98-75824 and from the Research Corporation RI0218. The simulations have been performed on IBM/SP2 in CINES, Montpellier, France and on CRAY/T3E in IDRIS, Paris, France.

REFERENCES

- [1] B.O. Mysen, *Structure and Properties of Silicate Melts* (Elsevier, Amsterdam, 1988).
- [2] G.E Brown, G.V. Gibbs, P.H Ribbe, *The American Mineralogist* **54**, 1044 (1969).
- [3] M. Taylor and G.E. Brown, *Geochim. et Cosmochim. Acta.* **43**, 61 (1978).
- [4] J. Zhao, P.H. Gaskell, L. Cormier, S.M. Bennington, *Physica B* **241** 906 (1998).
- [5] P. McMillan, B. Piriou and A. Navrotsky, *Geochim. et Cosmochim. Acta.* **46**, 2021 (1982).
- [6] Q. Williams and R. Jeanloz, *Science* **239**, 902 (1988).
- [7] C. Landron, B. Cote, D. Massiot, J.-P. Coutures and A.-M. Flank, *Phys. Stat. Sol. b* **171**, 9 (1992).
- [8] V. Petkov, Th. Gerber and B. Himmel, *Phys. Rev. B* **58**, 11 982 (1998).
- [9] V. Petkov, S.J.L. Billinge, S.D. Shastri and B. Himmel, *Phys. Rev. Letters* **85**, 3436 (2000).
- [10] Z. Wu, C. Romano, A. Marcelli, A. Mottana, G. Cibir, G. Della Ventura, G. Giuli, P. Courtial and D.B. Dingwell, *Phys. Rev. B* **60**, 9216 (1999).
- [11] C.I. Metzbacher, B.L. Serriff, J.S. Hartman and W.B. White, *J. Non-Cryst. Solids* **124** 194 (1990).
- [12] J.F. Stebbins and Z. Xu, *Nature* **390**, 60 (1997)
- [13] I. Farnan, *Nature* **390** 14 (1997).
- [14] P. Courtial and D.B. Dingwell, *Geochim. et Cosmochim. Acta* **59**, 3685 (1995).
- [15] I. Farnan and J.F. Stebbins, *Science* **265**, 1207 (1994).
- [16] J.F. Stebbins and I. Farnan, *Science* **255**, 586 (1992); I. Farnan and J.F. Stebbins, *J. Am. Chem. Soc.* **112**, 32 (1990).
- [17] D. Nevins and F.J. Spera, *American Mineralogist* **83** 1220 (1998).
- [18] C.A. Scamhorn and C.A. Angell, *Geochim. et Cosmochim. Acta* **55**, 721 (1990).
- [19] J.M. Delaye, V. Louis-Achille and D. Ghaleb, *J. Non-Cryst. Solids* **210**, 232 (1997).
- [20] C. Huang and A.N. Cormack, *J. Chem. Phys* **95** 3634 (1991).
- [21] J. Oviedo and J. Fernandez Sanz, *Phys. Rev. B* **58** 9047 (1998).
- [22] J. Sarnthein, A. Pasquarello, and R. Car, *Phys. Rev. B* **52**, 12 690 (1995)
- [23] M. Benoit, S. Ispas, P. Jund and R. Jullien, *Euro. Phys. J. B* **13**, 631 (2000).
- [24] R. Car and M. Parrinello, *Phys. Rev. Lett.* **55**, 2471 (1985).
- [25] CPMD Version 3.3, J. Hutter, A. Alavi, T. Deutsch, M. Bernasconi, St. Goedecker, D. Marx, M. Tuckerman and M. Parrinello, MPI für Festkörperforschung and IBM Research (1995-1999).
- [26] W. Kohn and L. Sham, *Phys. Rev.* **140 A**, 1133 (1965).
- [27] A.D. Becke, *Phys. Rev. A* **38**, 3098 (1988).
- [28] C. Lee, W. Yang and R.G. Parr, *Phys. Rev. B* **37**, 785 (1988).
- [29] G.B. Bachelet, D.R. Haman and M. Schlüter, *Phys. Rev. B* **26**, 4199 (1982).
- [30] N. Trouiller and J.L Martins, *Phys. Rev. B* **43**, 993 (1991).
- [31] S. Goedecker, M. Teter and J. Hutter, *Phys. Rev. B* **54**, 1703 (1996).
- [32] G. J. Martyna and M. E. Tuckerman, *J. Chem. Phys.* **110**, 2810 (1999).
- [33] I. Demachy and F. Volatron, *Euro.J. Inorg. Chem.* **1998**, 1015 (1998).
- [34] J.A. Dean, *Lange's Handbook of Chemistry* (McGraw-Hill inc., 1992).
- [35] B.W.H. van Beest, G.J. Kramer and R.A. van Santen, *Phys. Rev. Letters* **64**, 1955 (1990).

- [36] P. Jund and R. Jullien, *Phil. Mag. A* **79**, 223 (1999).
- [37] G. J. Martyna, M. E. Tuckerman and M. L. Klein, *J. Chem. Phys.* **97**, 2635 (1992).
- [38] G. J. Martyna, M. E. Tuckerman, D. J. Tobias and M. L. Klein, *Mol. Phys.* **87**, 1117 (1996).
- [39] M. E. Tuckerman and M. Parrinello, *J. Chem. Phys.* **101**, 1302 (1994).
- [40] J.M. Delaye, M. Benoit and D. Ghaleb, in preparation.
- [41] M.J. Toplis, S.C. Kohn, M.E. Smith and L.J.F. Poplett, *Am. Mineral.* **85**, 1556 (2000).
- [42] S.H. Risbud, R.J. Kirkpatrick, A.G. Tagliaiavore, B. Montez, *J. Am. Chem. Soc.* **70**, C10 (1987); R.K. Sato, P.F. McMillan, P. Dennison, R. Dupree, *Phys. Chem. Glasses* **32**, 149 (1991); R.K. Sato, P.F. McMillan, P. Dennison, R. Dupree, *J. Phys. Chem.* **95**, 4484 (1991).
- [43] J.F. Stebbins, S. Kroeker, S.K. Lee, T.J. Kiczinski, *J. Non-Cryst. Solids* **275**, 1 (2000).
- [44] E.R. Myers, V. Heine and M.T. Dove, *Phys. Chem. Minerals* **25** 457 (1998).
- [45] J. Klinowski, W.W. Carr, S.E. Tarling and P. Barnes, *Nature* **330**, 56 (1987); J. Stebbins, *Nature* **330**, 13 (1987).
- [46] S.K. Lee and J.F. Stebbins, *American Mineralogist* **84**, 937 (1999); J.F. Stebbins, S.K. Lee and J.V. Oglesby, *American Mineralogist* **84**, 983 (1999).
- [47] B. Himmel, J. Weigelt, Th. Gerber and M. Nofz, *J. Non-Cryst. Solids* **136**, 27 (1991).
- [48] J.A. Tossell and G. Saghi-Szabo, *Geochim. Cosmochim. Acta* **61**, 1171 (1997).
- [49] W.S. McDonald and D.W.J. Cruickshank, *Acta Cryst.* **62**, 37 (1967).
- [50] T. Uchino, M. Iwasaki, T. Sakka and Y. Ogata, *J. Phys. Chem.*, **95** 5455 (1991).
- [51] P. Minary, Z. Zhu and M. E. Tuckerman, to be submitted.
- [52] K. Vollmayr, PhD Thesis, University of Mainz, Germany (1995).
- [53] J. Horbach and W. Kob, *Phys. Rev. B* **60**, 3169 (1999).
- [54] L. Stixrude and M.S.T. Bukowinski, *Science* **250**, 4980 (1990).
- [55] N.P. Bansal and R.H. Doremus, *Handbook of Glass Properties* (Academic Press Inc., 1986).
- [56] R.B. Sosman, *The properties of Silica* (Chemical Catalog Company, New York, 1927).
- [57] P. Scheidler, W. Kob, A. Latz, J. Horbach and K. Binder, *Phys. Rev. B.* **63**, 104204 (2001).
- [58] O.V. Mazurin, M.V. Streltsina and T.P. Shvaiko-Shvaikovskaya, *Handbook of Glass Data*, (Elsevier, Amsterdam, 1983).

FIGURES

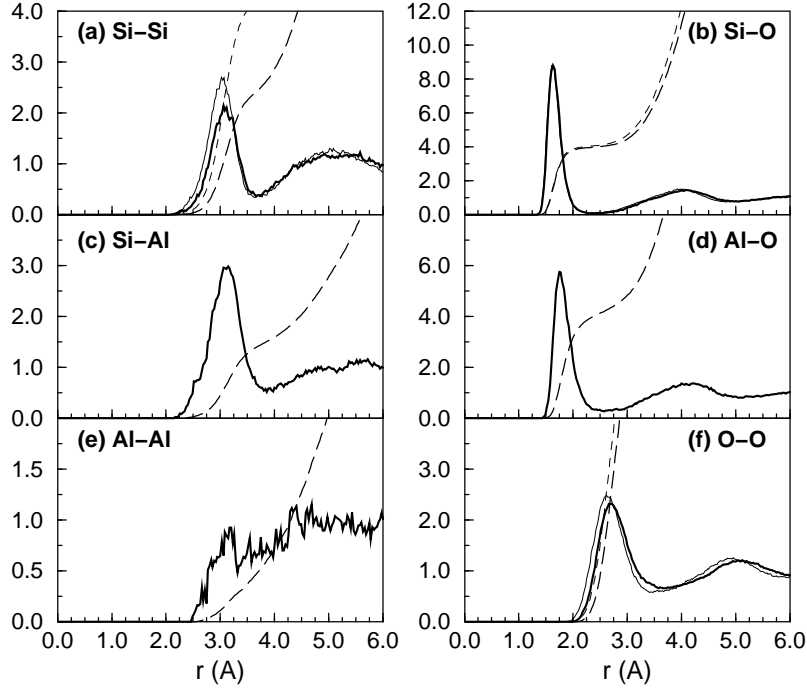


FIG. 1. Pair correlation functions of the network-forming atoms in the CAS system (bold lines) and in the silica system (thin lines). The integrated coordination numbers are also shown in dashed lines (bold and thin for CAS and SiO_2 , respectively).

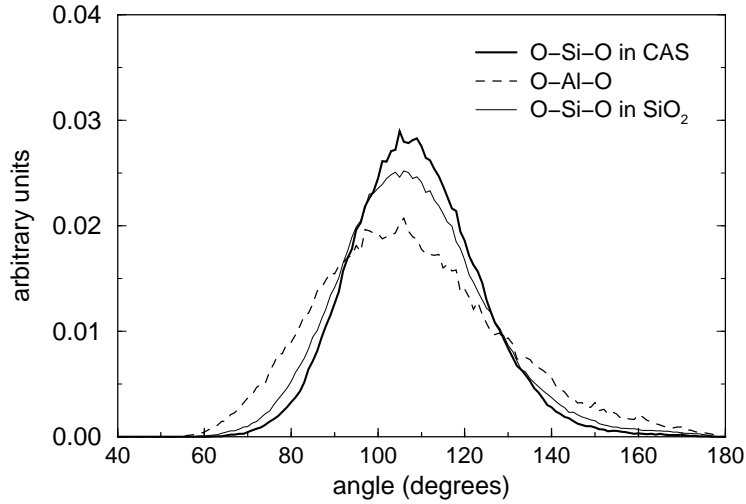


FIG. 2. Distribution of the O-Al-O angles in CAS (dashed line) and of the O-Si-O angles in CAS (bold line) and in SiO_2 (thin line).

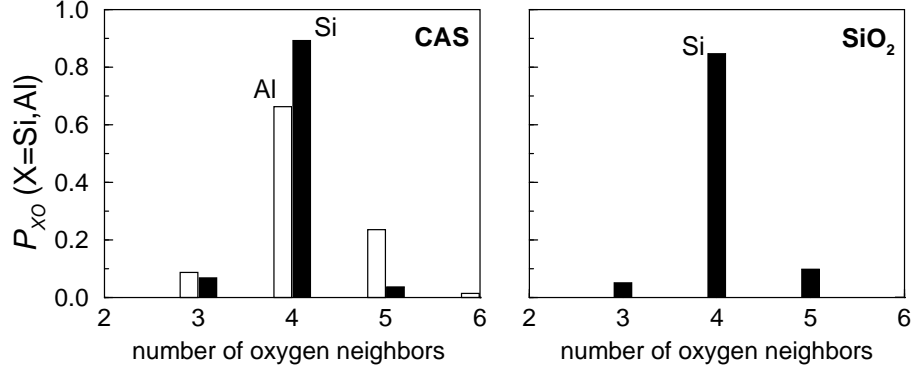


FIG. 3. Left graph: Histograms of $P_{XO}(N)$ ($X = Si, Al$), the probability of finding N oxygen atoms around the silicium (black) and aluminum (white) atoms in CAS. Right graph: Histogram of $P_{SiO}(N)$, the probability of finding N oxygen atoms around the silicium atoms in SiO₂.

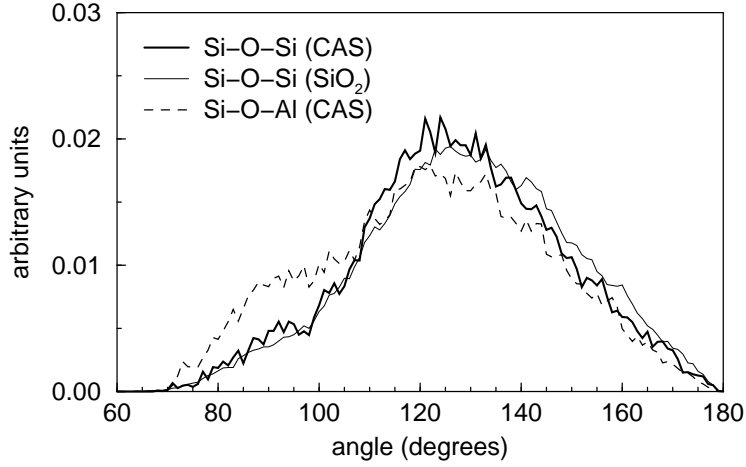


FIG. 4. Distribution of the Si-O-Si angles in CAS (bold line) and in SiO₂ (thin line) and distribution of the Si-O-Al angles in CAS (dashed line).

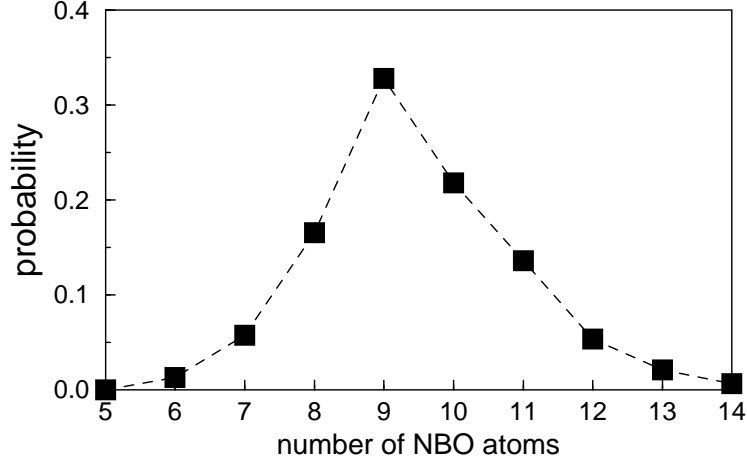


FIG. 5. Average distribution of the number of NBO atoms in the CAS system. The size of the symbols indicate the maximum error bar associated with the choice of distance cutoff for Al-O and Ca-O.

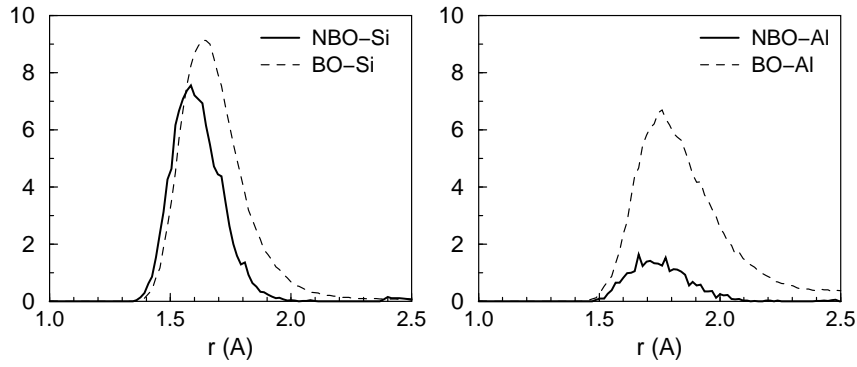


FIG. 6. Left graph: First peaks of the Si-BO (dashed line) and Si-NBO (bold line) pair correlation functions in CAS. Right graph: First peaks of the Al-BO (dashed line) and Al-NBO (bold line) pair correlation functions in CAS.

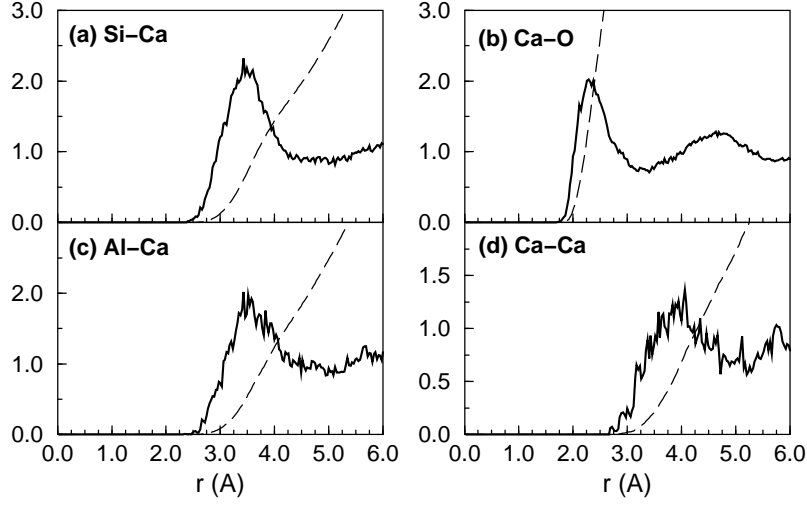


FIG. 7. Pair correlation functions of the calcium atoms in the CAS system and the corresponding integrated coordination numbers.

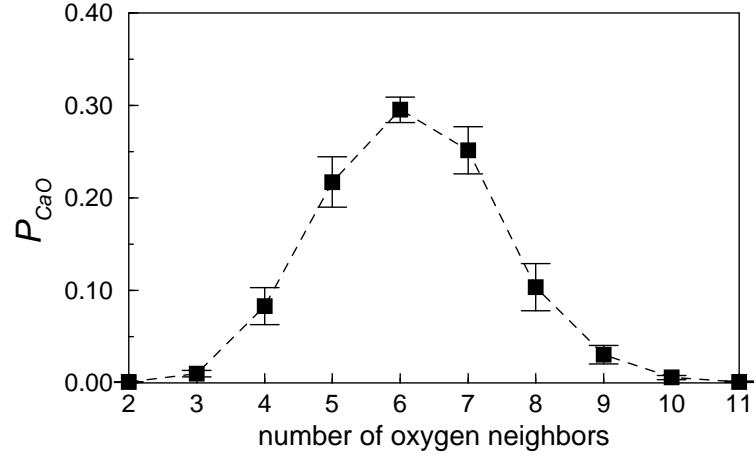


FIG. 8. Probability distribution, $P_{CaO}(N)$, for finding N oxygen atoms around a calcium atom in the CAS system. The error bars were estimated by bracketing the first minimum of $g_{Ca-O}(r)$ between statistical lower and upper bounds and varying the cutoff distance between these bounds.

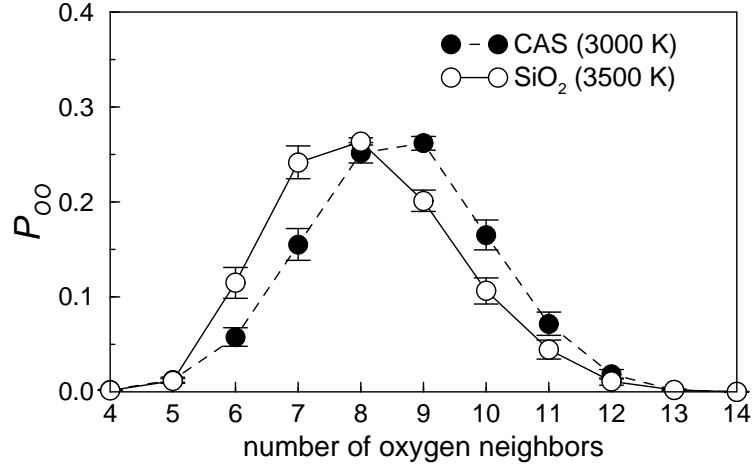


FIG. 9. Probability distribution, $P_{OO}(N)$, for finding N oxygens around a given oxygen atom in CAS and SiO₂. The error bars were estimated by bracketing the first minimum of $g_{O-O}(r)$ between statistical lower and upper bounds and varying the cutoff distance between these bounds.

TABLES

TABLE I. Results of distances and angles obtained from total energy calculations carried out on AlH_2OH , CaH_2 and CaH using the pseudo-potentials and the energy cutoffs given in the text. A Trouiller-Martins pseudo-potential was used for hydrogen. For these calculations, the reciprocal-space cluster boundary conditions method of Martyna and Tuckerman was employed [32]

AlH_2OH	This work	Ref. [33]
Al-O (\AA)	1.73(5)	1.711
Al-H ₁ (\AA)	1.56(4)	1.565
Al-H ₂ (\AA)	1.57(1)	1.575
O-H ₃ (\AA)	0.97(6)	0.956
$\widehat{\text{H}_1\text{AlH}_2}$	125.5	123.9
$\widehat{\text{AlOH}_3}$	122.3	122.3
CaH_2	This work	Ref. [34]
Ca-H ₁ (\AA)	2.03(0)	2.00
Ca-H ₂ (\AA)	2.03(1)	2.00
CaH	This work	Ref. [34]
Ca-H (\AA)	1.97(5)	2.00